Letter

Stripes and the emergence of charge π-phase shifts in isotropically paired systems

Jianhao Sun,[1] Tao Ying,[2,*] Richard T. Scalettar,[3,†] and Rubem Mondaini[4,5,‡]

[1]*Beijing Computational Science Research Center, Beijing 100193, China*
[2]*School of Physics, Harbin Institute of Technology, Harbin 150001, China*
[3]*Department of Physics and Astronomy, University of California, Davis, California 95616, USA*
[4]*Department of Physics, University of Houston, Houston, Texas 77004, USA*
[5]*Texas Center for Superconductivity, University of Houston, Houston, Texas 77204, USA*

(Received 27 February 2024; revised 18 September 2024; accepted 19 September 2024; published 3 October 2024)

The interplay of spin and motional degrees of freedom forms a key element in explaining stripe formation accompanied by sublattice reversal of local antiferromagnetic ordering in interacting fermionic models. A long-standing question aims to relate pairing to stripe formation, intending to discern the applicability of simple models that observe this phenomenon in understanding cuprate physics. By departing from fermionic statistics, we show that the formation of stripes is rather generic, allowing one to unveil its competition with superfluid behavior. To that end, we use a combination of numerical methods to solve a model of interacting hardcore bosons in ladder geometries, finding that once stripes are formed, either via external pinning or spontaneously, a sublattice reversal (π-phase shift) of *charge* ordering occurs, suppressing the superfluid weight. Lastly, we show that when the Cooper pairs are not local, as in the attractive Hubbard model with finite interactions, auxiliary-field quantum Monte Carlo calculations show evidence of fluctuating stripes, but these are seen to coexist with superfluidity. Our results corroborate the picture that static stripes cannot be reconciled with pairing, unlike the case of fluctuating ones.

DOI: 10.1103/PhysRevB.110.L161101

Introduction. Clarifying whether simplified lattice models capture the salient features of certain classes of high-temperature superconductors, such as the cuprates, has been at the forefront of scientific research in condensed matter physics for over three decades [1–3]. One of the aspects that complicates this quest is the absence of controlled analytical methods in dimensions larger than one that can tackle the solution of the corresponding Hamiltonians. Additionally, such a problem is even more elusive because of the small energy scales separating competing orders, creating challenges for numerical simulations.

While much remains to be settled, a recurring feature of existing calculations, which reproduces experimental observations [4], is the presence of charge stripes, wherein the doped holes unidirectionally condense over periodic regions in the lattice [5–23]. An additional aspect revealed by experimental and theoretical results is the emergence of a reversal of the sublattice magnetization across a stripe region in certain regimes of parameters, dubbed a π-phase shift (spin stripe). The common lore is that the high-temperature superconductors are characterized by intertwined orders [24], whose fate of competition/cooperation in suppressing/aiding the pairing properties is a question yet to be definitively answered.

Recently, however, large-scale numerical studies that combine constrained path quantum Monte Carlo [25] and density matrix renormalization group (DMRG) methods [26,27] to investigate the doped Hubbard model in large cylinders have started to converge toward the solution of this problem at the ground state [13,22,28]. Other approaches, such as unbiased auxiliary-field quantum Monte Carlo [14,15,29] or dynamical cluster approximations [18,21], are limited to low-but-finite temperatures, owing to the emergence of the sign problem [30,31]. Finite-temperature extensions of the DMRG method (minimally entangled typical thermal states [32,33]), however, allow one to bridge this gap, corroborating the emergence of charge and spin stripes over different temperature ranges [34].

In extensions to strongly coupled regimes, where a description in terms of a t-J model is appropriate [3], the formation of stripes is also observed. Still, the pairing in the hole-doped regime seems unattainable [35,36], defying the expectation that this particular model has "the right stuff" [37] to describe the cuprate physics. Note, however, that the inclusion of next-nearest-neighbor terms for both hoppings *and* exchange can change this picture, making superconductivity more robust in the hole-doped regime [38–42]. More recently, it has also been noted that observing phase reversal across hole-rich regions is not unique to repulsive models but is too seen on the charge degrees of freedom instead in the *attractive* Hubbard model [43]. Here, in the strong-coupling limit, the typical size of the Cooper pairs becomes increasingly small, asymptotically approaching a regime where a description of *repulsive* hardcore bosons (a composite fermionic pair) is relevant [44].

Many of the limitations that prevent the numerical study of the interplay of stripes and pairing do not occur if considering

*Contact author: taoying86@hit.edu.cn
†Contact author: scalettar@physics.ucdavis.edu
‡Contact author: rmondaini@uh.edu

the attractive Hubbard Hamiltonian [45] or repulsive hardcore bosons without frustration. Furthermore, from an experimental point of view, the study of the competition between pairing and stripes/charge ordering is friendlier in the scope of quantum emulators based on ultracold atoms in optical lattices since the temperature scales for the onset of isotropic (s-wave) superfluidity are higher, potentially allowing its observation within existing regimes accessible [46], even if not directly aiming to tackle the physics of the cuprate-like materials. In this paper, we take advantage of the capabilities of quantum simulations of such models; our key conclusions are: (i) In the strong coupling (bosonic) limit, *static* stripe density patterns emerge with doping; (ii) the charge density wave correlations are characterized by a phase shift across the stripes for sufficiently large intersite repulsion; (iii) regardless of the presence of this phase shift, superfluidity is suppressed by such *static* stripe formation. (iv) In contrast, at weaker coupling, the attractive fermionic Hubbard model, stripe formation is *not* inimical to pairing—quantum *fluctuating* stripes are central to coexistence with superconductivity. In addition, the simulations' accuracy allows us to quantify the energy differences of the competing phases precisely, something which is often referred to but not commonly evaluated.

Model. Our starting point is the attractive Fermi-Hubbard model [47–50]

$$\hat{\mathcal{H}} = -t \sum_{\langle i,j\rangle,\sigma} \hat{c}^{\dagger}_{i\sigma}\hat{c}_{j\sigma} + U\sum_{i}\hat{n}_{i\uparrow}\hat{n}_{i\downarrow} - \mu\sum_{i\sigma}\hat{n}_{i\sigma}, \qquad (1)$$

where $\hat{c}_{i\sigma}$ ($\hat{c}^{\dagger}_{i\sigma}$) annihilates (creates) an electron with spin σ in the site i of an $L_x \times L_y$ lattice and $\hat{n}_{i\sigma}$ is the corresponding number operator; t gives the hopping integral with on-site interactions $U < 0$, and the chemical potential μ regulates the fermionic density. For $|U|/t \gg 1$, the pairs induced by the attractive interactions turn local, describing a composite fermion satisfying the hardcore constraint: second-order perturbation theory recasts this Hamiltonian in terms of repulsive hardcore bosons in the presence of a rescaled chemical potential [44], $\hat{\mathcal{H}}' = -\frac{2t^2}{|U|}\sum_{\langle i,j\rangle}\hat{b}^{\dagger}_i\hat{b}_j + \frac{2t^2}{|U|}\sum_{\langle i,j\rangle}(\hat{n}'_i - 1/2)(\hat{n}'_j - 1/2) + (|U| - 2\mu)\sum_i(1-\hat{n}'_i)$, where $\hat{b}_i$ ($\hat{b}^{\dagger}_i$) is the ith site annihilation (creation) operator satisfying $[\hat{b}_i, \hat{b}^{\dagger}_j] = 0$ if $i \neq j$, while $\{\hat{b}_i, \hat{b}^{\dagger}_i\} = 1$, with the constraint $\hat{b}^{\dagger 2}_i = \hat{b}^2_i = 0$ [51]; $\hat{n}'_i = \hat{b}^{\dagger}_i\hat{b}_i$ is the associated number operator. This Hamiltonian for repulsively interacting hardcore bosons, generalized to allow the hopping amplitude to differ from the nearest-neighbor interaction strength, has been extensively studied [52–57]. With only nearest-neighbor interactions in a square lattice, the possible phases are either ordered solids (with different arrangements depending on the density $\langle\hat{n}'\rangle$) or a superfluid phase; their coexistence, i.e., a supersolid, has been ruled out [52,53]. At the first-order phase transition between the quantum solids and the superfluid phase with $\langle\hat{n}'\rangle$ close to 1/2, instability toward phase separation emerges, signaled by discontinuities in the equation of state [inset in Fig. 1(e)] and characterized by domain walls separated by antiphased checkerboard patterns [55]. This stripe formation can be explained via the contribution to the kinetic energy gain in second-order perturbation theory in the atomic limit [55,57] [see Fig. 1(b)].

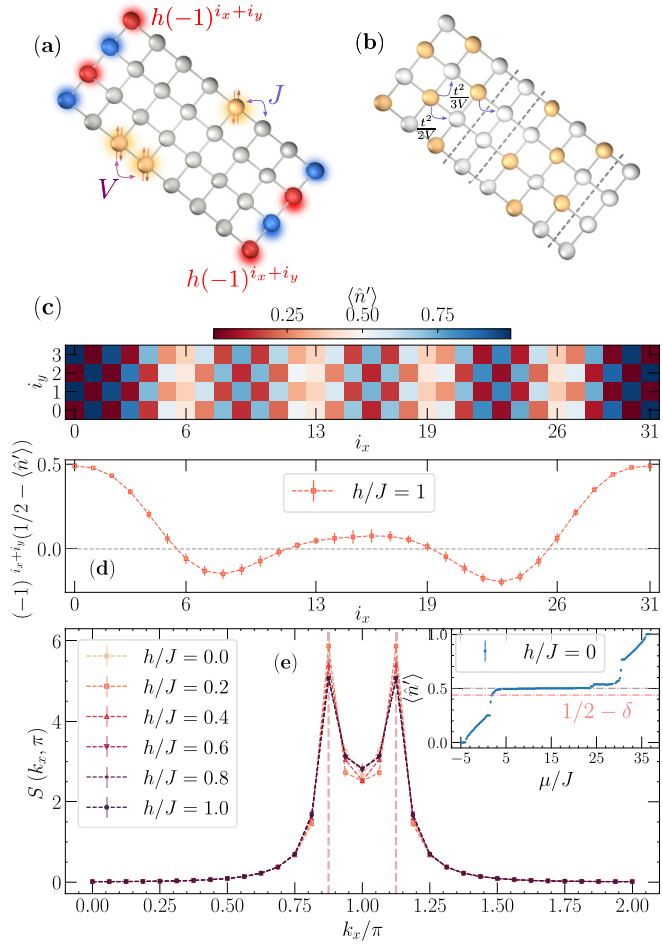

FIG. 1. (a) Schematic representation of the lattice with relevant terms of the hardcore boson Hamiltonian annotated, including staggered pinning potential at the edges with magnitude h. (b) Representation of the "charge π-phase shift" that emerges in the strongly interacting limit ($V/J \gg 1$), with contributions in second-order perturbation theory indicated. While the kinetic energy gains within a checkerboard domain are $\propto t^2/nV$ ($n = 2, 3$) for a given site, bosons can freely hop across the dashed lines marking the stripe locations. (c) Density profile in 32×4 ladder exhibiting four hole regions in its short direction; here $h/J = 1$. (d) The average staggered hole-density profile. (e) The density structure factor $S(k_x, \pi)$ shows robust peaks at $k_x = \pi(1 \pm 2\delta)$, $\delta = 1/16$, even in the absence of pinning potential ($h = 0$); the inset shows the phase separation characteristics for the studied densities emerging in the equation of state ($\langle n'\rangle$ vs μ). All data are obtained for $V/J = 8$.

Stripes in hardcore boson ladders. We start by characterizing the interplay between superfluidity and the emergence of stripes in ladder geometries. By breaking lattice rotational symmetry, they facilitate the manifestation of charge stripes along the short direction [11–15,19,22,23,58]. The Hamiltonian reads

$$\hat{\mathcal{H}}_{\rm hcb} = -J\sum_{\langle i,j\rangle}(\hat{b}^{\dagger}_i\hat{b}_j + \hat{b}^{\dagger}_j\hat{b}_i) + V\sum_{\langle i,j\rangle}\hat{n}'_i\hat{n}'_j - \mu\sum_i\hat{n}'_i, \qquad (2)$$

where we use the stochastic series expansion quantum Monte Carlo method [59–61] at sufficiently low temperatures T by setting $\beta \equiv 1/T = 2L_x$. Convergence is assisted towards the

formation of stripes when including a pinning staggered potential at the edges of the system [13,19,22], $h(-1)^{(i_x+i_y)}\hat{n}'_i$ for $i_x = 0$ and $L_x - 1$; see Fig. 1(a). Finally, we adjust the chemical potential μ such that the hole doping $\delta \equiv 1/2 - \langle \hat{n}' \rangle \simeq 1/16$. In the original picture of spinful fermions, this would correspond to the doping $\delta = 1/8$, often studied in the context of stripe formation in the repulsive Hubbard model [13,58] and where the "stripe anomaly" emerges in certain classes of cuprates (i.e., where stripes are most robust while suppressing bulk superconductivity [4,62]).

The site-resolved average density is shown in Fig. 1(c) on a 32×4 lattice with open (periodic) boundary conditions in the long (short) direction at the strongly interacting regime with $V/J = 8$, making immediately apparent the regions with increased hole density, periodically modulated along the ladder. Additionally, charge stripes separate regions where robust checkerboard patterns emerge. These two aspects can also be readily seen in the average staggered hole density, $(-1)^{i_x+i_y}(1/2 - \langle \hat{n}' \rangle)$, along the ladder [Fig. 1(d)] showing the region of antiphase, which is separated by hole-rich stripes wherein a node of the staggered hole density emerges.

To quantify the characteristic stripe wavelength, we compute the structure factor of the two-point, connected, density correlations,

$$S(\mathbf{k}) = \frac{1}{L_x L_y} \sum_{i,j} e^{i\mathbf{k}\cdot(\mathbf{r}_i - \mathbf{r}_j)} \langle (\hat{n}'_i - \langle \hat{n}'_i \rangle)(\hat{n}'_j - \langle \hat{n}'_j \rangle) \rangle, \qquad (3)$$

where we focus on the momenta $\mathbf{k} = (k_x, \pi)$. In the undoped case ($\delta = 0$), this quantity peaks at $\mathbf{k} = (\pi, \pi)$ owing to the robust checkerboard solid that emerges at such strong values of the nearest-neighbor interactions. In the presence of finite doping, we observe that its peak is now displaced to $k_x = \pi(1 \pm 2\delta)$ [Fig. 1(e)], a direct signature of the stripe formation and the antiphase the checkerboard domains exhibit across stripes [20,34]. Notably, for this case of hole-doping with $\delta = 1/16$, even without edge pinning potentials ($h = 0$), the π-phase striped charge density wave (CDW) is robust; see Supplemental Material (SM) [63] for a system-size analysis showing that this behavior persists for longer ladders but may exhibit competing stripe periodicities at wider ones.

Figure 2 shows how V/J affects this picture. The density inhomogeneity associated with the stripes is only seen for large values of V/J [inset Fig. 2(a)], a signature that just when doping the $\langle \hat{n}' \rangle = 1/2$ checkerboard solid, originally formed at $V/J \geqslant 2$ in the $\delta = 0$ regime, one may then observe charge stripes. Figure 2(b) shows that a robust density π-phase shift, i.e., $S(\pi, \pi) - S(\pi(1 \pm 2\delta), \pi) < 0$, is intimately tied to the stripe formation at large interactions. Lastly, we notice that increasing V/J, inducing the checkerboard solid formation, suppresses the superfluidity [Fig. 2(a)], quantified by $\rho_s = \langle W_x^2 + W_y^2 \rangle / (2\beta J)$, where $W_{x(y)}$ is the winding number of the bosonic world-lines in $x(y)$ directions [64]. The formation of sublattice reversal of checkerboard domains does not change this picture—a finite superfluid density is incompatible in this case as well. If enforcing the stripe emergence by an externally imposed potential [43,65,66] such anticorrelation between finite superfluidity and a robust manifestation of a π-phase shift persists; see the SM [63].

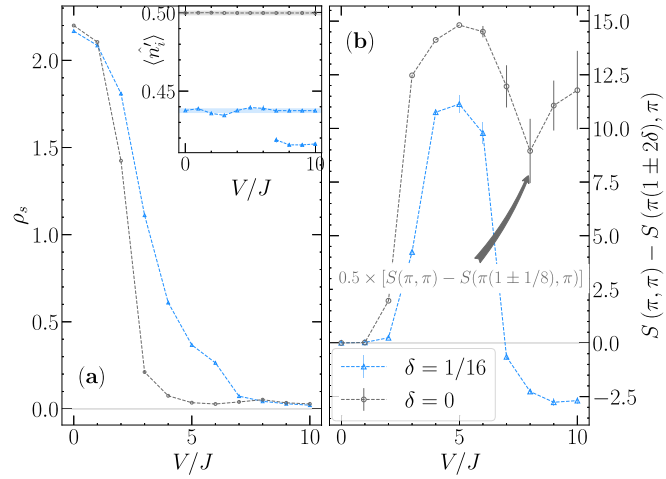

FIG. 2. (a) The superfluid weight vs interaction strength V with ($\delta = 1/16$) and without ($\delta = 0$) doping on the hardcore boson model shows that in the presence of stripes, $\rho_s \simeq 0$. These are seen in the inset, the shaded-horizontal area gives the average total density target, and the markers the calculated density—once charge stripes are formed for $V \gtrsim 7J$, these lead to a second lower density for $\delta = 1/16$ at certain regions. (b) The difference in the density structure factor for two values of k_x, π and $\pi(1 \pm 2\delta)$; when negative, it signals the emergence of stripes with antiphase density ordering—the undoped ($\delta = 0$) case is rescaled by 0.5 for easier visualization.

Stripes in $U < 0$ Fermi-Hubbard ladders. Having established that stripes naturally emerge in a model for hardcore bosons and that these compete with the superfluid properties once CDW domains are formed (with antiphase or not), we tackle the spinful attractive Hubbard model (1) to investigate if similar conclusions carry over. While its strongly interacting regime with increasingly local pairs is suggestive that similar results of the hardcore boson case would emerge, we argue below that much stronger quantum fluctuations lead to very different outcomes. In particular, the mapping to the hardcore boson Hamiltonian shows that in approaching the $|U|/t \gg 1$ limit, the corresponding hardcore boson model displays interaction strengths ($V = J$), which are not sufficient to induce a checkerboard solid at $\delta = 0$; see Fig. 2(b).

We start by showing in Fig. 3 the density structure factor [Eq. (3) with density operators for the fermionic case] with hole-doping $\delta = 1 - \langle \hat{n} \rangle \simeq 1/8$ and $|U|/t = 15$ on the same 32×4 ladder at $\beta t = 24$. We focus on a torus geometry (periodic boundaries in both directions) with an *antiphase* staggered potential $h(-1)^{i_x+i_y+i_x/8}\hat{n}_i$ applied at $i_x = 0, 8, 16, 24$; see Fig. 3(a). Imposition of a pinning potential provides a *useful tool* to filter a single stripe mode and assess its effect on pairing. Here, in particular, the competition of states that emerge at these low temperatures becomes clear: The simulations statistically converge such that $S(k_x, \pi)$ exhibits peaks at $k_x^{\text{peak}} = \pi$, $15\pi/16$, or $7\pi/8$ and their relative weight [i.e., the fraction of independent Markov chains (realizations) that converge to show a given peak in $S(k_x, \pi)$] can be tuned according to the magnitude of the pinning potential h; see Figs. 3(b)–3(d). The corresponding average energy per site $\langle \hat{\mathcal{H}} \rangle / (L_x L_y)$ (insets) explicitly depicts this competition, demonstrating that they are energetically very close. Such

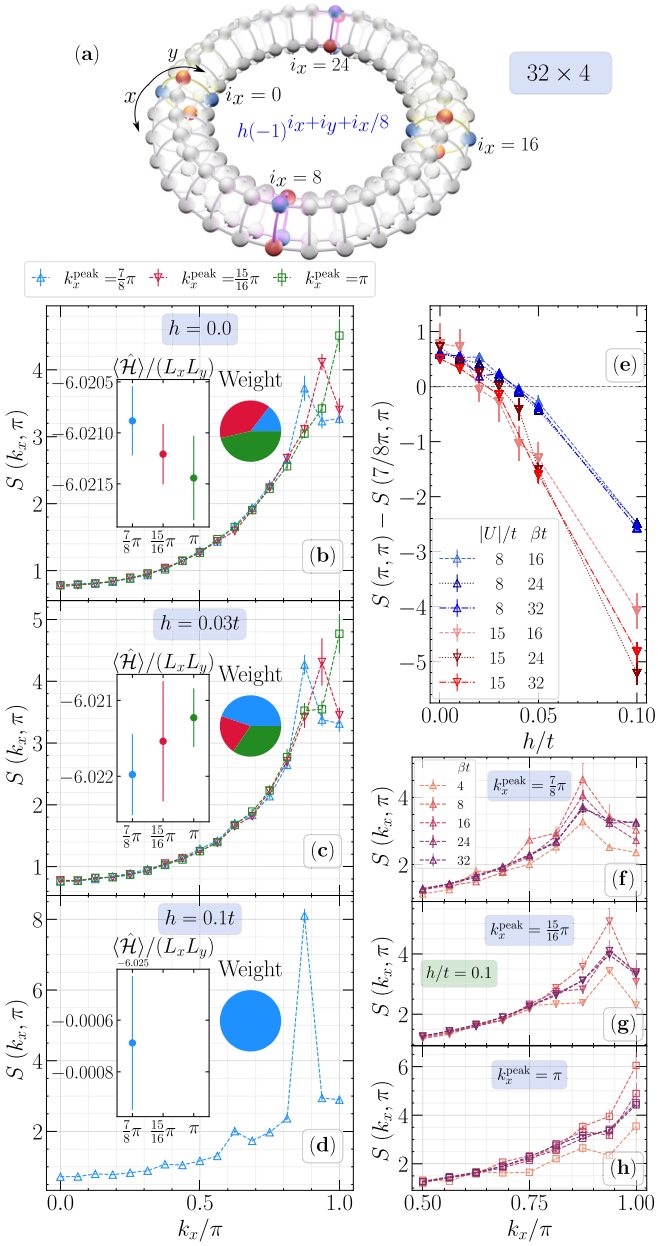

FIG. 3. (a) Schematic representation of the 32×4 ladder with periodic boundary conditions and the antiphase staggered pinning field at $i_x = 0, 8, 16, 24$. [(b)–(d)] Structure factor $S(k_x, \pi)$ for the *fermionic* model at $\beta t = 24$ with increasing magnitude of the modulated pinning potential $h/t = 0; 0.03$ and 0.1, respectively. Here, the realizations are filtered according to the peak location $k_x^{\rm peak}$—the pie chart gives the fraction of the total number of realizations exhibiting a given peak in $S(k_x, \pi)$ and the remaining inset the average energy per site for each corresponding k_x value. (e) The difference between the CDW structure factor and the one that gives a period-8 stripe averaged over *all* realizations: only after imposing a large pinning potential can a single-mode stripe be formed. [(f)–(h)] The temperature dependence of $S(k_x, \pi)$ with $h/t = 0.1$ for realizations exhibiting $k_{\rm peak} = \frac{7}{8}\pi$, $\frac{15}{16}\pi$, and π, respectively.

competition, associated with different stripe periodicities, is clear indication of their fluctuating nature.

Using $\Delta S \equiv S(\pi, \pi) - S(7\pi/8, \pi)$ as a proxy of robust antiphase period-8 stripe formation, Fig. 3(e) shows the

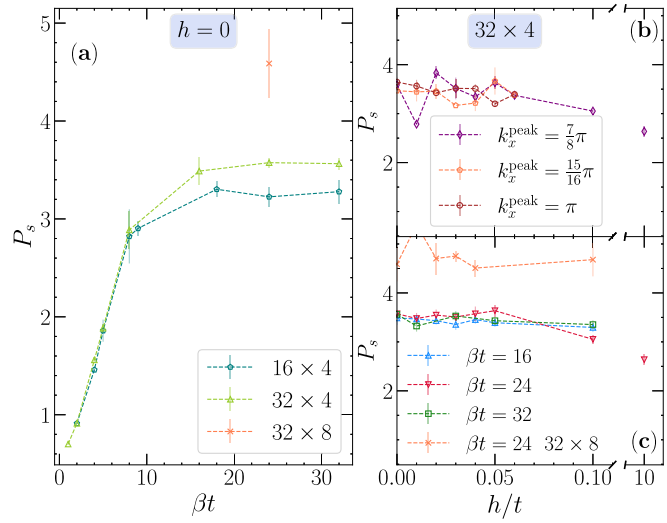

FIG. 4. (a) Saturation of the *s*-wave pair structure factor with the inverse temperature for three different system sizes without antiphase staggered pinning potentials $h(-1)^{i_x+i_y+i_x/8}\hat{n}_i$. The effect of h on the pairing for the 32×4 lattice, resolved by $k_x^{\rm peak}$ (b) or by temperature and system size (c). Note the broken axis with a value included at a large h, showing an overall reduction of the pairing once stripes become increasingly pinned. Data are shown for $|U|/t = 15$; imaginary-time discretization is $t\Delta\tau = 0.05$ as in Fig. 3.

necessity of including a pinning potential to tip the balance in favor of a single-mode stripe state with $\Delta S < 0$, also for smaller values of the attractive interactions strengths $|U|$ and temperatures. Focusing on the latter, we notice that in resolving $S(k_x, \pi)$ by the corresponding peak location across different realizations [Figs. 3(f)–3(h)], one can see relatively resilient peaks away from $k_x^{\rm peak} \neq \pi$ even at $T/t = 4$ for $h/t = 0.1$. This bodes well for observation in current experiments of trapped cold atoms emulating the attractive Hubbard model that has been shown to tackle a similar temperature range [46].

Lastly, we focus on the interplay of stripes and pairing, here quantified by the zero-momentum *s*-wave pair structure factor $P_s = \sum_{i,j} \langle \hat{\Delta}_i \hat{\Delta}_j^\dagger \rangle / (L_x L_y)$, where $\hat{\Delta}_i = \hat{c}_{i\uparrow}\hat{c}_{i\downarrow}$ annihilates a fermionic pair at site i. Low temperatures lead to a saturation of this quantity that is extensive with the system size [Fig. 4(a)], indicating an expected pairing long-range order when approaching the ground state [47]. While these results in the absence of pinning potential are not a guarantee that stripes are necessarily influencing them [see Fig. 3(b)], only a negligible decrease of the pairing is observed once small, single-mode stripe modulations are induced via the antiphase pinning potential at low temperatures [Fig. 4(c)], even if explicitly resolving the realizations that exhibit different $k_x^{\rm peak}$ in $S(k_x, \pi)$ [Fig. 4(b)]. The decrease is only substantial once one makes two orders of magnitude larger pinning potentials, leading to stripes that are increasingly static. This is what connects with the case of hardcore bosons, where stripes and superfluidity were incompatible, hinting that the larger quantum fluctuations when the stripes are not yet static in the fermionic case allow one to see concomitant manifestation of pairing and phase flip density modulations.

Summary and outlook. Disentangling the interplay of density modulations and pairing is at the core of understanding the physics of high-temperature superconductors. Here, we showed that stripes with antiphase checkerboard density are inimical to the superfluidity in interacting hard-core boson models: These can naturally form at strong interactions, leading to a stripe crystal that suppresses Bose-Einstein condensation. When these bosonic Cooper pairs are not tightly bound, stripe states emerge with more than one characteristic wave vector at low-T's [$k_x = \pi(1 \pm \delta)$ or $\pi(1 \pm \delta/2)$], consistent with fluctuating-stripe proposals, and are not seen to hurt the isotropic pairing significantly. Such a picture, here shown not to be necessarily tied to the repulsive Hubbard model, enlarges the scope in which multiple orders intertwine, opening the prospects of its observation in trapped ultracold atom experiments with controlled attractive interactions [46,67–69] where correlations of the *attractive* Hubbard model at different interaction strengths already identify regimes of tightly bound pairs. The accessible temperature range is close to the values that we show here are sufficient to see a π-phase shift across stripes. Systematic analysis of the correlations could provide signals of π ordering, as well as peaks at $\pi \pm 2\delta$ we find in Fig. 1(e).

Acknowledgments. T.Y. acknowledges support of the Natural Science Foundation of Heilongjiang Province (Grant No. YQ2023A004). R.M. acknowledges support from the T$_c$SUH Welch Professorship Award. R.T.S. is supported by the DOE Grant No. DE-SC0014671 funded by the U.S. Department of Energy, Office of Science. Numerical simulations were performed in the Tianhe-2JK at the Beijing Computational Science Research Center.

[1] D. J. Scalapino, E. Loh, and J. E. Hirsch, d-wave pairing near a spin-density-wave instability, Phys. Rev. B **34**, 8190 (1986).
[2] V. J. Emery, Theory of high-T_c superconductivity in oxides, Phys. Rev. Lett. **58**, 2794 (1987).
[3] F. C. Zhang and T. M. Rice, Effective Hamiltonian for the superconducting Cu oxides, Phys. Rev. B **37**, 3759 (1988).
[4] J. M. Tranquada, Cuprate superconductors as viewed through a striped lens, Adv. Phys. **69**, 437 (2020).
[5] J. Zaanen and O. Gunnarsson, Charged magnetic domain lines and the magnetism of high-T_c oxides, Phys. Rev. B **40**, 7391 (1989).
[6] D. Poilblanc and T. M. Rice, Charged solitons in the Hartree-Fock approximation to the large-U Hubbard model, Phys. Rev. B **39**, 9749 (1989).
[7] K. Machida, Magnetism in La_2 CuO_4 based compounds, Physica C: Supercond. **158**, 192 (1989).
[8] M. Kato, K. Machida, H. Nakanishi, and M. Fujita, Soliton lattice modulation of incommensurate spin density wave in two dimensional Hubbard model—A mean field study, J. Phys. Soc. Jpn. **59**, 1047 (1990).
[9] S. R. White and D. J. Scalapino, Density matrix renormalization group study of the striped phase in the 2D $t - J$ model, Phys. Rev. Lett. **80**, 1272 (1998).
[10] S. R. White and D. J. Scalapino, Energetics of domain walls in the 2D $t - J$ model, Phys. Rev. Lett. **81**, 3227 (1998).
[11] C.-C. Chang and S. Zhang, Spin and charge order in the doped Hubbard model: Long-wavelength collective modes, Phys. Rev. Lett. **104**, 116402 (2010).
[12] B.-X. Zheng and G. K.-L. Chan, Ground-state phase diagram of the square lattice Hubbard model from density matrix embedding theory, Phys. Rev. B **93**, 035126 (2016).
[13] B.-X. Zheng, C.-M. Chung, P. Corboz, G. Ehlers, M.-P. Qin, R. M. Noack, H. Shi, S. R. White, S. Zhang, and G. K.-L. Chan, Stripe order in the underdoped region of the two-dimensional Hubbard model, Science **358**, 1155 (2017).
[14] E. W. Huang, C. B. Mendl, S. Liu, S. Johnston, H.-C. Jiang, B. Moritz, and T. P. Devereaux, Numerical evidence of fluctuating stripes in the normal state of high-T_c cuprate superconductors, Science **358**, 1161 (2017).
[15] E. W. Huang, C. B. Mendl, H.-C. Jiang, B. Moritz, and T. P. Devereaux, Stripe order from the perspective of the Hubbard model, npj Quantum Mater. **3**, 22 (2018).
[16] T. I. Vanhala and P. Törmä, Dynamical mean-field theory study of stripe order and d-wave superconductivity in the two-dimensional Hubbard model, Phys. Rev. B **97**, 075112 (2018).
[17] H.-C. Jiang and T. P. Devereaux, Superconductivity in the doped Hubbard model and its interplay with next-nearest hopping t', Science **365**, 1424 (2019).
[18] P. Mai, S. Karakuzu, G. Balduzzi, S. Johnston, and T. A. Maier, Intertwined spin, charge, and pair correlations in the two-dimensional Hubbard model in the thermodynamic limit, Proc. Natl. Acad. Sci. USA **119**, e2112806119 (2022).
[19] H. Xu, H. Shi, E. Vitali, M. Qin, and S. Zhang, Stripes and spin-density waves in the doped two-dimensional Hubbard model: Ground state phase diagram, Phys. Rev. Res. **4**, 013239 (2022).
[20] H. Schlömer, A. Bohrdt, L. Pollet, U. Schollwöck, and F. Grusdt, Robust stripes in the mixed-dimensional $t - J$ model, Phys. Rev. Res. **5**, L022027 (2023).
[21] P. Mai, N. S. Nichols, S. Karakuzu, F. Bao, A. Del Maestro, T. A. Maier, and S. Johnston, Robust charge-density-wave correlations in the electron-doped single-band Hubbard model, Nat. Commun. **14**, 2889 (2023).
[22] H. Xu, C.-M. Chung, M. Qin, U. Schollwöck, S. R. White, and S. Zhang, Coexistence of superconductivity with partially filled stripes in the Hubbard model, Science **384**, eadh7691 (2024).
[23] S. Jiang, D. J. Scalapino, and S. R. White, Density matrix renormalization group based downfolding of the three-band Hubbard model: Importance of density-assisted hopping, Phys. Rev. B **108**, L161111 (2023).
[24] E. Fradkin, S. A. Kivelson, and J. M. Tranquada, *Colloquium:* Theory of intertwined orders in high temperature superconductors, Rev. Mod. Phys. **87**, 457 (2015).
[25] S. Zhang, J. Carlson, and J. E. Gubernatis, Constrained path quantum Monte Carlo method for fermion ground states, Phys. Rev. Lett. **74**, 3652 (1995).
[26] S. R. White, Density matrix formulation for quantum renormalization groups, Phys. Rev. Lett. **69**, 2863 (1992).

[27] S. R. White, Density-matrix algorithms for quantum renormalization groups, Phys. Rev. B **48**, 10345 (1993).

[28] M. Qin, C.-M. Chung, H. Shi, E. Vitali, C. Hubig, U. Schollwöck, S. R. White, and S. Zhang (Simons Collaboration on the Many-Electron Problem), Absence of superconductivity in the pure two-dimensional Hubbard model, Phys. Rev. X **10**, 031016 (2020).

[29] T. Liu, D. Jost, B. Moritz, E. W. Huang, R. Hackl, and T. P. Devereaux, Tendencies of enhanced electronic nematicity in the Hubbard model and a comparison with Raman scattering on high-temperature superconductors, Phys. Rev. B **103**, 134502 (2021).

[30] E. Y. Loh, J. E. Gubernatis, R. T. Scalettar, S. R. White, D. J. Scalapino, and R. L. Sugar, Sign problem in the numerical simulation of many-electron systems, Phys. Rev. B **41**, 9301 (1990).

[31] R. Mondaini, S. Tarat, and R. T. Scalettar, Quantum critical points and the sign problem, Science **375**, 418 (2022).

[32] S. R. White, Minimally entangled typical quantum states at finite temperature, Phys. Rev. Lett. **102**, 190601 (2009).

[33] E. M. Stoudenmire and S. R. White, Minimally entangled typical thermal state algorithms, New J. Phys. **12**, 055026 (2010).

[34] A. Wietek, Y.-Y. He, S. R. White, A. Georges, and E. M. Stoudenmire, Stripes, antiferromagnetism, and the pseudogap in the doped Hubbard model at finite temperature, Phys. Rev. X **11**, 031007 (2021).

[35] S. R. White and D. J. Scalapino, Competition between stripes and pairing in a $t-t'-J$ model, Phys. Rev. B **60**, R753 (1999).

[36] S. Jiang, D. J. Scalapino, and S. R. White, Ground-state phase diagram of the $t-t'-J$ model, Proc. Natl. Acad. Sci. USA **118**, e2109978118 (2021).

[37] D. Scalapino, Does the Hubbard model have the right stuff? in *Proceedings of the International School of Physics*, edited by R. Broglia and J. Schrieffer (North-Holland, Amsterdam, 1994).

[38] S. Gong, W. Zhu, and D. N. Sheng, Robust d-wave superconductivity in the square-lattice $t-J$ model, Phys. Rev. Lett. **127**, 097003 (2021).

[39] H.-C. Jiang and S. A. Kivelson, High temperature superconductivity in a lightly doped quantum spin liquid, Phys. Rev. Lett. **127**, 097002 (2021).

[40] H.-C. Jiang, S. A. Kivelson, and D.-H. Lee, Superconducting valence bond fluid in lightly doped eight-leg $t-J$ cylinders, Phys. Rev. B **108**, 054505 (2023).

[41] X. Lu, F. Chen, W. Zhu, D. N. Sheng, and S.-S. Gong, Emergent superconductivity and competing charge orders in hole-doped square-lattice $t-J$ model, Phys. Rev. Lett. **132**, 066002 (2024).

[42] F. Chen, F. D. M. Haldane, and D. N. Sheng, D-wave and pair-density-wave superconductivity in the square-lattice $t-J$ model arXiv:2311.15092.

[43] T. Ying, R. T. Scalettar, and R. Mondaini, π phase shift across stripes in a charge density wave system, Phys. Rev. B **105**, 115116 (2022).

[44] R. Micnas, J. Ranninger, and S. Robaszkiewicz, Superconductivity in narrow-band systems with local nonretarded attractive interactions, Rev. Mod. Phys. **62**, 113 (1990).

[45] So long as the single-particle part is the same for both spin species.

[46] T. Hartke, B. Oreg, C. Turnbaugh, N. Jia, and M. Zwierlein, Direct observation of nonlocal fermion pairing in an attractive Fermi-Hubbard gas, Science **381**, 82 (2023).

[47] R. T. Scalettar, E. Y. Loh, J. E. Gubernatis, A. Moreo, S. R. White, D. J. Scalapino, R. L. Sugar, and E. Dagotto, Phase diagram of the two-dimensional negative-U Hubbard model, Phys. Rev. Lett. **62**, 1407 (1989).

[48] A. Moreo and D. J. Scalapino, Two-dimensional negative-U Hubbard model, Phys. Rev. Lett. **66**, 946 (1991).

[49] T. Paiva, R. R. dos Santos, R. T. Scalettar, and P. J. H. Denteneer, Critical temperature for the two-dimensional attractive Hubbard model, Phys. Rev. B **69**, 184501 (2004).

[50] R. A. Fontenele, N. C. Costa, R. R. dos Santos, and T. Paiva, Two-dimensional attractive Hubbard model and the BCS-BEC crossover, Phys. Rev. B **105**, 184502 (2022).

[51] E. Lieb, T. Schultz, and D. Mattis, Two soluble models of an antiferromagnetic chain, Ann. Phys. (NY) **16**, 407 (1961).

[52] R. T. Scalettar, G. G. Batrouni, A. P. Kampf, and G. T. Zimanyi, Simultaneous diagonal and off-diagonal order in the Bose-Hubbard Hamiltonian, Phys. Rev. B **51**, 8467 (1995).

[53] F. Hébert, G. G. Batrouni, R. T. Scalettar, G. Schmid, M. Troyer, and A. Dorneich, Quantum phase transitions in the two-dimensional hardcore boson model, Phys. Rev. B **65**, 014513 (2001).

[54] G. Schmid, S. Todo, M. Troyer, and A. Dorneich, Finite-temperature phase diagram of hard-core bosons in two dimensions, Phys. Rev. Lett. **88**, 167208 (2002).

[55] P. Sengupta, L. P. Pryadko, F. Alet, M. Troyer, and G. Schmid, Supersolids versus phase separation in two-dimensional lattice bosons, Phys. Rev. Lett. **94**, 207202 (2005).

[56] S. Wessel and M. Troyer, Supersolid hard-core bosons on the triangular lattice, Phys. Rev. Lett. **95**, 127205 (2005).

[57] X. Zhu, S. Dong, Y. Lin, R. Mondaini, H. Guo, S. Feng, and R. T. Scalettar, Self-organized bosonic domain walls, Phys. Rev. Res. **2**, 013085 (2020).

[58] E. W. Huang, T. Liu, W. O. Wang, H.-C. Jiang, P. Mai, T. A. Maier, S. Johnston, B. Moritz, and T. P. Devereaux, Fluctuating intertwined stripes in the strange metal regime of the Hubbard model, Phys. Rev. B **107**, 085126 (2023).

[59] A. W. Sandvik, Stochastic series expansion method with operator-loop update, Phys. Rev. B **59**, R14157 (1999).

[60] A. Albuquerque, F. Alet, P. Corboz, P. Dayal, A. Feiguin, S. Fuchs, L. Gamper, E. Gull, S. Gürtler, A. Honecker *et al.*, The ALPS project release 1.3: Open-source software for strongly correlated systems, J. Magn. Magn. Mater. **310**, 1187 (2007).

[61] B. Bauer, L. D. Carr, H. G. Evertz, A. Feiguin, J. Freire, S. Fuchs, L. Gamper, J. Gukelberger, E. Gull, S. Guertler *et al.*, The ALPS project release 2.0: Open source software for strongly correlated systems, J. Stat. Mech.: Theory Exp. (2011) P05001.

[62] M. Hücker, M. v. Zimmermann, G. D. Gu, Z. J. Xu, J. S. Wen, G. Xu, H. J. Kang, A. Zheludev, and J. M. Tranquada, Stripe order in superconducting La_{2-x} Ba_x CuO_4 ($0.095 \leqslant x \leqslant 0.155$), Phys. Rev. B **83**, 104506 (2011).

[63] See Supplemental Material at http://link.aps.org/supplemental/10.1103/PhysRevB.110.L161101 for more details on the stripe

emergence for hardcore boson doping in the first model (as opposed to hole doping) and corresponding finite-size effects in the quantities investigated, which includes Refs. [4,22,43,44,52–56,65,66,70–84].

[64] E. L. Pollock and D. M. Ceperley, Path-integral computation of superfluid densities, Phys. Rev. B **36**, 8343 (1987).

[65] R. Mondaini, T. Ying, T. Paiva, and R. T. Scalettar, Determinant quantum Monte Carlo study of the enhancement of d-wave pairing by charge inhomogeneity, Phys. Rev. B **86**, 184506 (2012).

[66] C. Chen, Z. Fan, R. Ma, Y. Pan, Y. Liang, B. Huang, and T. Ma, Stripe order manipulated dominant pairing symmetry in the Hubbard model, Phys. Rev. B **109**, 045101 (2024).

[67] D. Mitra, P. T. Brown, E. Guardado-Sanchez, S. S. Kondov, T. Devakul, D. A. Huse, P. Schauß, and W. S. Bakr, Quantum gas microscopy of an attractive Fermi–Hubbard system, Nat. Phys. **14**, 173 (2018).

[68] P. T. Brown, E. Guardado-Sanchez, B. M. Spar, E. W. Huang, T. P. Devereaux, and W. S. Bakr, Angle-resolved photoemission spectroscopy of a Fermi–Hubbard system, Nat. Phys. **16**, 26 (2020).

[69] C. F. Chan, M. Gall, N. Wurz, and M. Köhl, Pair correlations in the attractive Hubbard model, Phys. Rev. Res. **2**, 023210 (2020).

[70] C. Chen, P. Zhong, X. Sui, Y. Liang, S. Hu, T. Ma, H.-Q. Lin, and B. Huang, Charge stripe manipulation of superconducting pairing symmetry transition, arXiv:2304.14254.

[71] S. Robaszkiewicz, R. Micnas, and K. A. Chao, Thermodynamic properties of the extended Hubbard model with strong intra-atomic attraction and an arbitrary electron density, Phys. Rev. B **23**, 1447 (1981).

[72] R. Mondaini, G. G. Batrouni, and B. Grémaud, Pairing and superconductivity in the flat band: Creutz lattice, Phys. Rev. B **98**, 155142 (2018).

[73] X. Jin, Y. Liu, R. Mondaini, and M. Rigol, Charge excitations across a superconductor-insulator transition, Phys. Rev. B **106**, 245117 (2022).

[74] M. Kohno and M. Takahashi, Magnetization process of the spin-$\frac{1}{2}$XXZ models on square and cubic lattices, Phys. Rev. B **56**, 3212 (1997).

[75] A. Kuklov, N. Prokof'ev, and B. Svistunov, Weak first-order superfluid-solid quantum phase transitions, Phys. Rev. Lett. **93**, 230402 (2004).

[76] S. V. Isakov, S. Wessel, R. G. Melko, K. Sengupta, and Y. B. Kim, Hard-core bosons on the kagome lattice: Valence-bond solids and their quantum melting, Phys. Rev. Lett. **97**, 147202 (2006).

[77] P. Zanardi and N. Paunković, Ground state overlap and quantum phase transitions, Phys. Rev. E **74**, 031123 (2006).

[78] L. Campos Venuti and P. Zanardi, Quantum critical scaling of the geometric tensors, Phys. Rev. Lett. **99**, 095701 (2007).

[79] P. Zanardi, P. Giorda, and M. Cozzini, Information-theoretic differential geometry of quantum phase transitions, Phys. Rev. Lett. **99**, 100603 (2007).

[80] W.-L. You, Y.-W. Li, and S.-J. Gu, Fidelity, dynamic structure factor, and susceptibility in critical phenomena, Phys. Rev. E **76**, 022101 (2007).

[81] M.-F. Yang, Ground-state fidelity in one-dimensional gapless models, Phys. Rev. B **76**, 180403(R) (2007).

[82] C. N. Varney, K. Sun, M. Rigol, and V. Galitski, Interaction effects and quantum phase transitions in topological insulators, Phys. Rev. B **82**, 115125 (2010).

[83] C. J. Jia, B. Moritz, C.-C. Chen, B. S. Shastry, and T. P. Devereaux, Fidelity study of the superconducting phase diagram in the two-dimensional single-band Hubbard model, Phys. Rev. B **84**, 125113 (2011).

[84] R. Mondaini, P. Nikolić, and M. Rigol, Mott-insulator–to–superconductor transition in a two-dimensional superlattice, Phys. Rev. A **92**, 013601 (2015).